Cappuccini, F., Eldh, T., Bruder, D., Gereke, M., Jastrow, H., Schulze-Osthoff, K., Fischer, U., Köhler, D., Stuschke, M., Jendrossek, V.

New insights into the molecular pathology of radiation-induced pneumopathy

(2011) Radiotherapy and Oncology, 101 (1), pp. 86-92.

New insights into the molecular pathology of radiation-induced pneumopathy

Federica Cappuccini[1*], Therese Eldh[2*], Dunja Bruder[3], Marcus Gereke[3], Holger Jastrow[4], Klaus Schulze-Osthoff[5], Ute Fischer[6], David Köhler[7], Martin Stuschke[8], Verena Jendrossek[1]

[1]Institute of Cell Biology (Cancer Research), University Hospital Essen, Essen, Germany; [2]Department of Radiation Oncology, University of Tübingen, Tübingen, Germany; [3]Immune regulation group, Helmholtz Centre for Infection Research, Braunschweig, Germany; [4]Department of Anatomy, University Hospital Essen, Essen, Germany; [5]Interfaculty Institute for Biochemistry, University of Tübingen, Tübingen, Germany; [6]University Childrens Hospital Düsseldorf, Department for Pediatric Oncology, Hematology and Clinical Immunology, Düsseldorf, Germany; [7]Department of Anesthesiology and Intensive Care Medicine, University of Tübingen, Tübingen, Germany; [8]Department of Radiotherapy, University Hospital Essen, Essen, Germany

* both authors contributed equally

Corresponding author:

Verena Jendrossek, Institute of Cell Biology (Cancer Research), University Hospital Essen, Virchowstrasse 173, 45122 Essen, Germany; Phone: +49-201-7233380; Fax: +49-201-7235904; E-mail: verena.jendrossek@uni-due.de.

Total number of pages: 13

Total number of words: 4365 including abstract, acknowledgements, figure legends and references

Total number of tables: 0

Total number of figures: 4

Running head: molecular pathology of radiation-induced pneumopathy

Key words: thorax irradiation, pneumonitis, fibrosis, apoptosis, lipid loaded macrophages, T-lymphocytes, albumin leakage, Rag-2 deficient mice

Abstract:

Background and Purpose: Pneumonitis and fibrosis constitute dose-limiting side effects of thorax or total body irradiation. An improved understanding of the underlying mechanisms is a prerequisite for the development of effective radioprotective strategies. Here we characterized the behaviour of resident and immune cells in a murine model of radiation-induced pneumopathy.

Materials and Methods: Wild type (WT) or RAG-2 deficient C57BL/6 mice received 15 Gray of (hemi)-thorax irradiation in a single dose. Bronchoalveolar lavage fluid (BALF) and lung tissue were collected at defined time points post-irradiation for determination of apoptosis, microvascular injury, and histological and immunohistochemical analyses.

Results: Higher albumin levels and increased apoptosis were detected in the BALF 21 days after irradiation, indicative for delayed damage to resident cells. Irradiation also induced time-dependent changes in the BALF cytokine profile, the recruitment of activated T-cells into the lung and the formation of lipid-loaded resident cells. Lung fibrosis occurred earlier in RAG-$2^{-/-}$ mice, which lack mature T and B cells, compared to WT mice.

Conclusions: Thorax irradiation triggers a delayed disturbance of tissue integrity and lipid metabolism in the lung. Activated T lymphocytes infiltrating the lung tissue upon thorax irradiation participate in the protection of the lung from radiation-induced fibrosis.

Introduction

Radiotherapy is a mainstay for the treatment of cancer patients. Unfortunately, the high intrinsic sensitivity of normal tissues often precludes the application of curative radiation doses. As an example, radiation-induced pneumopathy is still a major obstacle in the treatment of thorax-associated neoplasms [1-4]. Consequently, the combination of radiotherapy with drugs protecting the normal lung tissue from the toxic effects of radiotherapy could be an effective strategy for improving treatment outcome. However, no biology-based strategy to specifically prevent or treat radiation-induced pneumopathy has been approved to date, so that a symptomatic anti-inflammatory therapy remains standard of care [5]. Although considerable progress has been made during the last decade in defining disease biomarkers [5, 6] and involved molecular factors, e.g. transforming growth factor ß (TGF-ß), intracellular adhesion molecule 1, platelet derived growth factor, as well as the death receptor CD95 and its ligand [7-10], the network of pathophysiologic events linking acute tissue damage to chronic inflammation and fibrosis requires further definition. Because of the complexity of the involved cellular systems and soluble factors these investigations can only be performed *in vivo*. Here, we characterize radiation-induced changes in resident cells and recruited immune cells upon thorax irradiation and defined the role of lymphocytes for fibrosis development in a murine model.

Material and Methods

Mouse strains

Eight-to-twelve weeks-old C57BL/6 wild-type mice (WT; Charles River, Sulzfeld, Germany) or with a homozygous deletion of recombination-activating gene 2 (RAG-2$^{-/-}$) [11] were enrolled in the study. Mice were housed in a standard barrier facility at a room temperature of 20-22°C with a 12-hour light/dark cycle. Food and drinking water were provided ad libitum. All protocols were approved by the Universities Animal Protection Boards in conjunction with the Regierungspräsidium Tübingen (R 1/04) and the Landesamt für Natur, Umwelt und Verbraucherschutz Nordrhein-Westfalen (G 1094/09).

Irradiation

Mice were anesthetized with 2% isoflurane, placed in holders and irradiated with a single dose of 0 Gy (sham) or 15 Gy over their right hemithorax, using a linear accelerator (dose rate 4.7 Gy/min). Alternatively, whole thorax irradiation (15 Gy) was performed with a Cobalt-60 source (dose rate

0.5 Gy/min). Non-irradiated parts of the body were shielded with 6 cm of lead. Mice were sacrificed at days 1, 3, 10, 21, 42, or 168 post-irradiation and bronchoalveolar lavage fluid or lung tissue were collected for further analysis.

Bronchoalveolar lavage (BAL)

To obtain BAL fluid (BALF), a horizontal incision was made in the dissected tracheal tube. A syringe needle was connected and fixed by two surgical knots and the lungs were lavaged three times with 0.5 mL PBS. All fluid collected from one mouse was pooled, centrifuged and aliquots of the supernatant were stored by -20 ˚C for determination of albumin, cytokines, and caspase-3/7-activity. Cell pellets of each treatment group were pooled and cell differentiation was performed in Advia 120 automated flow cytometry (Siemens Healthcare Diagnostics, Eschborn, Germany).

Determination of albumin leakage

Albumin levels in thawed BALF were determined using the Albumin ELISA Quantitation Kit Mouse (Bethyl Laboratories, Montgomery, USA) according to manufacturer's instructions. Shortly, 100 µL 1:500 and 1:1000 PBS-diluted BALF as well as standard probes were added in duplicates to the wells coated with capture antibody and incubated for 1 h. Upon development, absorbance was recorded at 450 nm in a microtiter plate reader (Anthos Labtec, Krefeld, Germany).

Determination of apoptosis

Active caspase-3/7 was detected in BALF using Caspase-Glo 3/7 Kit (Promega, Mannheim, Germany). 10 µL undiluted BALF or 10 µL serum, diluted 1:2 in Caspase-Glo dilution buffer, were incubated with the caspase substrate DEVD-luciferin and luciferase reagent for 3 h at room temperature. The sample luminescence was measured and calculated as the increase relative to untreated controls.

Myeloperoxidase assay

Pulmonary innate immune cell recruitment was quantified in lungs perfused with PBS using a myeloperoxidase (MPO)-assay as described elsewhere [12]. In this assay, MPO activity is determined using a colorimetric reaction with *o*-dianisidine. Absorbance was measured at 450 nm and results presented as difference in optical density over 5 min (ΔOD).

Cytokine array

The cytokine pattern in BALF was analyzed using the Proteome Profiler Mouse Cytokine Array, Panel A Kit (R&D, Wiesbaden-Nordenstadt, Germany) according to manufacturer's instructions. For each time point, BALF from irradiated or sham-irradiated WT mice was pooled. Pixel density

of the spots with bound cytokines/chemokines was analyzed using Photoshop. Mean pixel density values from duplicate spots for the treatment groups were compared with the values of the sham irradiated control group as follows: Δpixel density = pixel density 15 Gy-group – pixel density 0 Gy-group.

Immunohistochemistry

Mice were euthanized and lungs were isolated without or after intratracheal perfusion with 4% (wt/vol) paraformaldehyde (PFA) in PBS (pH 7.2) and fixed overnight in the same solution. Upon dehydration, lungs were embedded in paraffin and sectioned in 5 µm slices.

For *histopathological evaluation*, sections were stained with H&E or Masson-Goldner Trichrome staining, respectively, and scored for the number of fibrotic foci. At least 3 random sections of 2 different lungs per group were examined by FC blinded for the background and treatment of the mice.

For *determination of apoptosis*, deparaffinised and rehydrated lung sections were placed on coated microscope slides (Superfrost Plus) and steam boiled in 1 L citrate buffer pH 6. Sections were sequentially blocked for 20 min with Rotiblock, 3% skim milk, and 10% normal pork serum with 0.2% Triton (PBS/S/T). Blocked sections were incubated with active caspase-3 antibody in PBS/S/T over night at 4 °C. Endogenous peroxidase was blocked with 3% H_2O_2. Caspase-3 was detected using an anti-rabbit secondary IgG antibody in PBS/S/T, Streptavidin AP Complex ready to use, and Fast red staining (Roche, Mannheim, Germany). Stained sections were counterstained with hematoxylin, rinsed in running tap water, and covered with Aquatex.

For *electron microscopy*, tissue was fixed with 2.5% glutaraldehyde in 0.1M cacodylate, contrasted with OsO4, uranylacetate and lead citrate and investigated on a Zeiss EM902. Images were acquired on a MegaViewII slow-scan-CCD camera using ITEM® 5.0 software (Soft-imaging-systems, Münster, Germany).

Semithin sections (0.5 µm) of glutaraldhyde-fixed tissue were dried and stained with toluidine blue 1%, methylene blue 1% and Azur-II 1% solution in water pH 8.0 plus 1% sodium tetraborate.

Phenotyping of T-lymphocyte subpopulations

The lungs were digested in 0.2 mg/mL Collagenase D/Dispase at 37 °C and the cell suspension filtered (100 µm cell strainer) and subsequently centrifuged by 1200 rpm. Mononuclear cells were then isolated over Ficoll and stained with either IL-17 or FoxP3 in combination with CD4 and CD25 antibodies. For the **IL-17 staining** the cells were stimulated with 1 mg/mL PMA, 1 mg/mL

Ionomycin and 5 mg/mL Brefeldin for 6 h and stained with CD4-FITC antibody (1:1200; e-Bioscience, San Diego, USA) and CD25-Bio antibody (1:500; Becton Dickinson, Heidelberg, Germany) for 10 min and subsequently with Streptavidin (SAv)-APC secondary antibody (1:100; Becton Dickinson, Heidelberg, Germany) for 10 min. Next, the cells were stained for 30 min with IL-17 antibody solution (1:500; Beckton Dickinson, Heidelberg, Germany) after 2% PFA fixation and 0.1% NP40 detergent treatment, and analyzed by flow cytometry (FACSCalibur, Beckton & Dickinson, Heidelberg, Germany). For **FOXP3 staining** cells were incubated with CD4 and CD25 as well as SAv-APC secondary antibody, as above. The cells were fixed with BD Cytofix buffer, incubated with FOXP3 antibody (1:150; e-Bioscience, San Diego, USA) for 30 min in the dark and analyzed by flow cytometry (FACSCalibur, Becton Dickinson, Heidelberg, Germany).

Data analysis

If not otherwise indicated, analyses were made in triplicate and mean values were used for analysis of standard deviation (SD), standard error (SE), and statistical significance (ANOVA statistical test; student t-test) using GraphPad InStat (La Jolla, USA).

Results

We have recently shown that the death receptor CD95 and its ligand participate in the pathogenesis of radiation-induced pneumonitis in mice [9]. Because of the role of CD95 and CD95-ligand in apoptosis regulation, we analysed whether single dose hemithorax irradiation would trigger apoptotic cell death during evolving pneumonitis. Interestingly, apoptosis was clearly detected in the tissue of irradiated and shielded lungs (Fig. 1A) and in BALF collected from the whole lung (Fig. 1B) of WT mice at day 21 post-irradiation (15 Gy). No such increase was observed at day 1 post-irradiation (not shown) or in control mice (0 Gy). Apoptotic cells were primarily bronchiolar epithelial cells. Further investigations are ongoing to define additional cell type/s that may undergo apoptosis in the lumen. Moreover, we found increased levels of albumin in the BALF of irradiated WT mice at day 21 post-irradiation when compared to control mice (Fig. 1C). Interestingly, at the same time point we also observed radiation-induced changes in the morphology of resident lung cells. In particular, irradiation triggered the formation of lipid-loaded macrophages and endothelial cells (Fig. 2) suggesting a disturbance of lipid metabolism in the irradiated lung tissue. These data clearly demonstrate that thorax irradiation is associated with a delayed damage to resident lung cells and loss of barrier function.

Because the CD95/CD95-ligand system has an additional role in immune cell attraction, we next examined the recruitment of inflammatory cells into the lung tissue. As shown in Fig. 3A, hemithorax irradiation triggered the recruitment of neutrophils, lymphocytes, monocytes and basophils to the lung of WT mice. These results were corroborated by a significant increase in MPO-activity in the lung tissue by day 21 post-irradiation, which is indicative for the presence of neutrophils and monocytes (Fig. 3B). Immune cells recruitment was also associated with time-dependent changes in macrophage- and lymphocyte-associated cytokines/chemokines present in the BALF of irradiated mice. As shown in Fig. 3C, we observed increased levels of macrophage-colony stimulating factor (M-CSF) and macrophage chemoattractant protein-1 (MCP-1) at day 3 and 21 post-irradiation, respectively. M-CSF is a key regulator of proliferation, survival and differentiation of monocytes/macrophages, whereas MCP-1 functions in the attraction of monocytes, granulocytes and lymphocytes. Thus, both chemokines may promote the influx of immune cells, particularly macrophages, into the irradiated lungs by day 21. Also, the levels of macrophage inflammatory protein (MIP)-1ß and MIP-2 were found increased particularly at day 21 post-irradiation, although the MIP-2 increase was more prominent. Both proteins participate in the activation of granulocytes and the synthesis of proinflammatory cytokines and may thus foster inflammation-associated lung damage. Moreover, MCP-1 and MIPs have suggested profibrotic effects [13].

Surprisingly, the levels of several cytokines involved in the recruitment, proliferation and/or activation of $CD4^+$ T-cells, particularly T_H17 cells, were also largely increased by day 21 post-irradiation in the BALF of irradiated mice (Fig. 3D). We therefore analysed whether lung irradiation would affect the composition of T-lymphocyte subsets recruited to the irradiated lung tissue. Interestingly, thorax irradiation triggered a time-dependent increase in the fraction of $CD4^+/CD25^+$ activated T lymphocytes until day 21 post-irradiation, among them IL-17^+ cells and $FOXP3^+$ cells (Fig. 3E). The results however, did not reach statistical significance, probably due to low sample number. Nevertheless, those data suggested that specific T-lymphocyte subsets may participate in the regulation of tissue inflammation and repair induced by thorax irradiation. To gain more insight into the role of T-lymphocytes we analysed in a last set of experiments whether the late effects of thorax irradiation would be altered in RAG-$2^{-/-}$ mice. Due to a total inability to initiate V(D)J rearrangement, RAG-$2^{-/-}$ mice fail to generate mature T- and B-lymphocytes [11]. For these investigations we used whole thorax irradiation with 15 Gy instead of hemithorax irradiation as this treatment modality has been described to readily induce lung fibrosis in C57BL/6 mice [14, 15]. In contrast, in our hands hemithorax irradiation with 12.5 to 15 Gy was below the threshold for lung fibrosis. A pronounced collagen deposition was only observed upon hemithorax irradiation with 22.5 Gy (Eldh et al., 2011 unpublished data), a dose that was however linked with a mortality rate of 15%. Surprisingly, enhanced collagen deposition and increased numbers of fibrotic foci were detected by day 168 after whole thorax irradiation in the lung tissue of RAG-$2^{-/-}$ mice when compared to irradiated WT mice (Fig. 4). This reveals an increased sensitivity of RAG-$2^{-/-}$ mice to radiation-induced lung fibrosis.

Discussion

Our study demonstrates that thorax irradiation affects tissue integrity and triggers specific time-dependent changes in resident lung cells and recruited inflammatory cells. Importantly, we provide evidence that mature lymphocytes participate in the protection against radiation-induced lung fibrosis.

At first, we observed increased apoptosis in the lung tissue and enhanced albumin leakage into the BALF of irradiated WT mice 21 days post-irradiation pointing towards disturbance of the lungs barrier function. These findings support earlier reports about delayed death or impairment of resident epithelial and/or endothelial cells leading to a loss of barrier function in the irradiated lung tissue [5, 16, 17]. Interestingly, increased apoptosis was observed in both, the irradiated and the shielded lung tissue. This is reminiscent of earlier findings about spreading of radiation-induced

lung inflammation to non-irradiated areas of the lung tissue [5, 9] and suggests that apoptosis in the shielded lungs is a result of a secondary systemic effect induced by circulating immune cells or soluble proapoptotic factors, e.g. death receptor ligands.

Furthermore, we demonstrate the formation of lipid-loaded resident cells upon hemithorax irradiation. The appearance of foamy macrophages in the BALF of irradiated C57BL/6 mice has already been observed in an earlier study [17]. However, here we show for the first time that radiation-induced formation of lipid droplets is not restricted to BALF-macrophages but is also found in tissue macrophages as well as in resident endothelial cells. This suggests a more general disturbance of lipid metabolism in the irradiated lung. Though, the functional relevance of lipid droplet formation for radiation-induced pneumopathy remains to be defined. We speculate that similar to the foamy macrophages in atherosclerotic lesions, lipid-loaded macrophages in the irradiated lung tissue may represent an alternative activation state, characteristic for deregulated immune homeostasis and repair.

Thorax irradiation not only affected the macrophage phenotype present in the lung tissue, but also triggered the recruitment of various immune cells into the lung by day 21, among them monocytic cells, neutrophils, basophils and lymphocytes. Immune cells recruitment was associated with characteristic changes in macrophage-associated and $CD4^+$ T-lymphocytes/T_H17-associated cytokines and chemokines present in the BALF of irradiated mice. Up to now, elevated plasma levels of TGF-ß and interleukin-6 (IL-6), as well as decreased levels of IL-10, have been proposed as biomarkers for radiation-induced pneumopathy in patients [18, 19]. Moreover, a time-dependent increase in tissue levels of TGF-ß, tumor necrosis factor-α, IL-1ß, and IL-6 mRNA as well as of MCP-1 and 3 and MIP-1γ proteins levels has been described in irradiated mice [13, 17, 20]. However, here we show for the first time that thorax irradiation triggers prominent changes in the protein levels of the macrophage-associated and $CD4^+$ T-lymphocytes/T_H17-associated cytokines MIP-2, IL-16, IL-17, IL-23 and IL27 in the BALF. In line with this observation, we found an increased recruitment of activated $CD4^+$ T-lymphocytes into the lung tissue until day 21 post-irradiation. It is known from preclinical and clinical studies that T-lymphocytes constitute a significant part of immune cells infiltrating the lung tissue upon thorax irradiation [13, 17, 21, 22]. Moreover, increased numbers of activated T-lymphocytes in the BALF were found to correlate with the onset of radiation-induced pneumonitis [23]. Here we show for the first time that $CD4^+CD25^+IL\text{-}17^+$ and $CD4^+CD25^+Foxp3^+$ expressing cells are recruited to the lung tissue of irradiated mice. Even more important, the lack of mature T- and B-cells increased the sensitivity of RAG-$2^{-/-}$ mice to radiation-induced lung fibrosis. This observation suggests that lymphocytes

recruited to the lung tissue are key players in the regulation of lung inflammation and fibrosis in response to thorax irradiation and that they may be required to keep in check cells of the innate immune system, e.g. macrophages, or of the adaptive immune system which otherwise may exert tissue-destructive effects [24]. In support of this hypothesis, selective depletion of $CD4^+$ T-cells in irradiated rats caused a significant reduction in the thickening of lung parenchyma during the pneumonitic phase [25]. The obvious dual role of lymphocytes for radiation-induced pneumopathy is reminiscent of results obtained in the model of bleomycin-induced pneumopathy [26, 27] and requires further definition.

In conclusion, thorax irradiation triggers a delayed disturbance of tissue integrity and the formation of lipid-loaded resident cells. Activated T lymphocytes constitute a significant part of immune cells infiltrating the lung tissue upon thorax irradiation and are an important cellular component in the control of radiation-induced late adverse effects. The role of lipid-loaded macrophages and of $CD4^+CD25^+$IL-17^+ and $CD4^+CD25^+Foxp3^+$ T-cell subsets, presumably T_H17-cells and regulatory T-cells, for radiation-induced pneumopathy is under current investigation.

Acknowledgements

We thank Dr. Ali Sak, Michael Groneberg, Eva Gau, Dorothea Schünke, Dr. Ralph Waldschütz and Dr. Gretel Chometon-Luthe, for excellent technical support. The work was supported by grants of the DFG (GK794) to TE and the Deutsche Krebshilfe/Mildred-Scheel-Stiftung (107388) to VJ.

Conflict of Interest Statement

No conflict of interest does exist for any of the authors.

References

[1] Trott, KR, Herrmann, T, Kasper, M. Target cells in radiation pneumopathy. Int J Radiat Oncol Biol Phys 2004;58:463-469.
[2] Kristensen, CA, Nottrup, TJ, Berthelsen, AK, et al. Pulmonary toxicity following IMRT after extrapleural pneumonectomy for malignant pleural mesothelioma. Radiother Oncol 2009;92:96-99.
[3] Guckenberger, M, Baier, K, Polat, B, et al. Dose-response relationship for radiation-induced pneumonitis after pulmonary stereotactic body radiotherapy. Radiother Oncol 2010;97:65-70.
[4] Borst, GR, Ishikawa, M, Nijkamp, J, et al. Radiation pneumonitis in patients treated for malignant pulmonary lesions with hypofractionated radiation therapy. Radiother Oncol 2009;91:307-313.
[5] Graves, PR, Siddiqui, F, Anscher, MS, Movsas, B. Radiation pulmonary toxicity: from

mechanisms to management. Semin Radiat Oncol 2010;20:201-207.
[6] De Ruysscher, D, Houben, A, Aerts, HJ, et al. Increased (18)F-deoxyglucose uptake in the lung during the first weeks of radiotherapy is correlated with subsequent Radiation-Induced Lung Toxicity (RILT): a prospective pilot study. Radiother Oncol 2009;91:415-420.
[7] Hallahan, DE, Virudachalam, S. Intercellular adhesion molecule 1 knockout abrogates radiation induced pulmonary inflammation. Proc Natl Acad Sci U S A 1997;94:6432-6437.
[8] Abdollahi, A, Li, M, Ping, G, et al. Inhibition of platelet-derived growth factor signaling attenuates pulmonary fibrosis. J Exp Med 2005;201:925-935.
[9] Heinzelmann, F, Jendrossek, V, Lauber, K, et al. Irradiation-induced pneumonitis mediated by the CD95/CD95-ligand system. J Natl Cancer Inst 2006;98:1248-1251.
[10] Anscher, MS, Peters, WP, Reisenbichler, H, Petros, WP, Jirtle, RL. Transforming growth factor beta as a predictor of liver and lung fibrosis after autologous bone marrow transplantation for advanced breast cancer. N Engl J Med 1993;328:1592-1598.
[11] Shinkai, Y, Rathbun, G, Lam, KP, et al. RAG-2-deficient mice lack mature lymphocytes owing to inability to initiate V(D)J rearrangement. Cell 1992;68:855-867.
[12] Eckle, T, Fullbier, L, Wehrmann, M, et al. Identification of ectonucleotidases CD39 and CD73 in innate protection during acute lung injury. J Immunol 2007;178:8127-8137.
[13] Johnston, CJ, Williams, JP, Okunieff, P, Finkelstein, JN. Radiation-induced pulmonary fibrosis: examination of chemokine and chemokine receptor families. Radiat Res 2002;157:256-265.
[14] Moore, BB, Hogaboam, CM. Murine models of pulmonary fibrosis. Am J Physiol Lung Cell Mol Physiol 2008;294:L152-160.
[15] McDonald, S, Rubin, P, Chang, AY, et al. Pulmonary changes induced by combined mouse beta-interferon (rMuIFN-beta) and irradiation in normal mice--toxic versus protective effects. Radiother Oncol 1993;26:212-218.
[16] Molteni, A, Moulder, JE, Cohen, EF, et al. Control of radiation-induced pneumopathy and lung fibrosis by angiotensin-converting enzyme inhibitors and an angiotensin II type 1 receptor blocker. Int J Radiat Biol 2000;76:523-532.
[17] Chiang, CS, Liu, WC, Jung, SM, et al. Compartmental responses after thoracic irradiation of mice: strain differences. Int J Radiat Oncol Biol Phys 2005;62:862-871.
[18] Zhao, L, Wang, L, Ji, W, et al. Elevation of plasma TGF-beta1 during radiation therapy predicts radiation-induced lung toxicity in patients with non-small-cell lung cancer: a combined analysis from Beijing and Michigan. Int J Radiat Oncol Biol Phys 2009;74:1385-1390.
[19] Arpin, D, Perol, D, Blay, JY, et al. Early variations of circulating interleukin-6 and interleukin-10 levels during thoracic radiotherapy are predictive for radiation pneumonitis. J Clin Oncol 2005;23:8748-8756.
[20] Rube, CE, Wilfert, F, Palm, J, et al. Irradiation induces a biphasic expression of pro-inflammatory cytokines in the lung. Strahlenther Onkol 2004;180:442-448.
[21] Roberts, CM, Foulcher, E, Zaunders, JJ, et al. Radiation pneumonitis: a possible lymphocyte-mediated hypersensitivity reaction. Ann Intern Med 1993;118:696-700.
[22] Nakayama, Y, Makino, S, Fukuda, Y, Min, KY, Shimizu, A, Ohsawa, N. Activation of lavage lymphocytes in lung injuries caused by radiotherapy for lung cancer. Int J Radiat Oncol Biol Phys 1996;34:459-467.
[23] Morgan, GW, Breit, SN. Radiation and the lung: a reevaluation of the mechanisms mediating pulmonary injury. Int J Radiat Oncol Biol Phys 1995;31:361-369.
[24] Para, AE, Bezjak, A, Yeung, IW, Van Dyk, J, Hill, RP. Effects of genistein following fractionated lung irradiation in mice. Radiother Oncol 2009;92:500-510.
[25] Westermann, W, Schobl, R, Rieber, EP, Frank, KH. Th2 cells as effectors in postirradiation pulmonary damage preceding fibrosis in the rat. Int J Radiat Biol 1999;75:629-638.
[26] Luzina, IG, Todd, NW, Iacono, AT, Atamas, SP. Roles of T lymphocytes in pulmonary

fibrosis. J Leukoc Biol 2008;83:237-244.
[27] Pociask, DA, Chen, K, Choi, SM, Oury, TD, Steele, C, Kolls, JK. gammadelta T cells attenuate bleomycin-induced fibrosis through the production of CXCL10. Am J Pathol 2011;178:1167-1176.

Figure Legends

Figure 1: Hemithorax irradiation induces delayed apoptosis and disturbance of barrier function in C57BL/6 mice. WT mice received 0 Gy (sham-control) or 15 Gy hemithorax irradiation. **A)** Determination of apoptosis by immunohistochemistry: Prominent active caspase-3-positive signals at day 21 are only visible in the lung tissue of irradiated mice but not in the lung tissue of sham-controls**. B)** Detection of active caspase-3/7 in the BALF: The levels of active caspase-3/7 were significantly increased at day 21 in the BALF of irradiated mice compared to sham-controls. The results show mean values±SD (n=3) of relative luminescence units (RLU; * significant difference; $p \leq 0.05$; t-test with two-tail p-value). **C)** Detection of albumin leakage into the BALF by ELISA: Increased albumin leakage was detected at day 21 post-irradiation in irradiated mice when compared to sham controls. Shown are mean values±SD (n=3; *significant difference $p \leq 0.05$; one-tailed t-test).

Figure 2: Irradiation triggers the formation of lipid-loaded resident lung cells: WT mice received 0 Gy (sham-control) or 15 Gy hemithorax irradiation. **A)** Electron microscopy picture of a lipid-loaded endothelial cell at day 21 post-irradiation (white arrows: lipid droplets; scale bar: 2 µm). **B)** Semi-thin section (0,5 µm) showing a lipid-loaded macrophage at day 42 post-irradiation (black arrows: lipid droplets; magnification x100; scale bar: 10 µm). **C)** Quantification of lipid-loaded macrophages at day 21 and day 42 in semi-thin slices. Data represent the mean percentage±SD in lipid-loaded macrophages on the total macrophage number (=100%) obtained in ≥ 3 different sections/value; 2 mice were analyzed per condition (*significant difference $p \leq 0.05$; two-tailed unpaired t-test).

Figure 3: Thorax irradiation triggers the recruitment of immune cells: WT mice received 0 Gy (sham-control) or 15 Gy hemithorax irradiation. BALF or lung tissue were collected at the indicated time points and analysed for the presence of immune cells and cytokines/chemokines as indicated. **A)** *BALF cell differentiation using Advia 120*: Increased numbers of neutrophils, lymphocytes, monocytes and basophils are found in the BALF of irradiated mice compared to that of sham-irradiated control mice by day 21 post-irradiation. Data represent mean values obtained in pooled BALF of 3 mice/ group. **B)** *Determination of myeloperoxidase (MPO)-activity in the lung tissue by*

a spectrophotometric assay: Irradiation of the right hemithorax of C57BL/6 mice triggers a significant increase in MPO-levels 21 days post-irradiation. The results are presented as difference in MPO units (ΔOD; mean values±SD; n=6; *significant difference $p \leq 0.05$; one-tailed paired t-test). **C and D)** *Determination of time-dependent changes in monocyte/macrophage-specific and lymphocyte/T_H17-specific cytokines/chemokines in BALF by a Cytokine Proteome Array*: Results are illustrated as difference in pixel intensity (Δpixel intensity) = pixel intensity of irradiated mice – pixel intensity of sham-irradiated mice. BALF of 3 mice/group was pooled for one experiment. Representative results from one of three similar experiments are shown. C) Hemithorax irradiation triggered prominent time-dependent changes in MCP-1 and MIP-2 protein levels, and minor changes in MIP-1ß and M-CSF levels. D) Irradiation triggered time-dependent changes in all lymphocyte/T_H17-associated cytokines investigated. **E)** *Determination of T_H17 cells and Treg cell in lung tissue by flow cytometry.* Hemithorax irradiation triggers a slight but not significant increase in the fraction of $CD4^+/CD25^+$ T cells, $CD4^+/CD25^+/IL\text{-}17^+$ T-cells, and $CD4^+/CD25^+/Foxp3^+$ T-cells until day 21. Shown are mean values±SEM of three independent experiments. Cells of 3 (experiments 1 and 2) or 5 mice/group (experiment 3) were pooled. (*significant difference $p \leq 0.05$; one-tailed t-test).

Figure 4: Lack of mature T and B lymphocytes sensitizes to radiation-induced lung fibrosis: RAG-$2^{-/-}$ and C57BL/6 wild type mice received 0 Gy (sham control) or 15 Gy whole thorax irradiation. Histological analysis was performed in H&E or Masson-Goldner Trichrome stained lung sections 24 weeks after irradiation (magnification x10; scale bars: 100 µm). **A)** Representative light microscopy pictures of H&E stained lung sections. **B)** Representative light microscopy pictures of Masson-Goldner Trichrome stained lung sections; **C)** Quantification of fibrotic foci in irradiated mice 24 weeks after irradiation. Data represent the mean number of foci counted in ≥ 3 sections (2 mice per condition); *significant difference $p \leq 0.05$; two-tailed unpaired t-test).

Figure 1

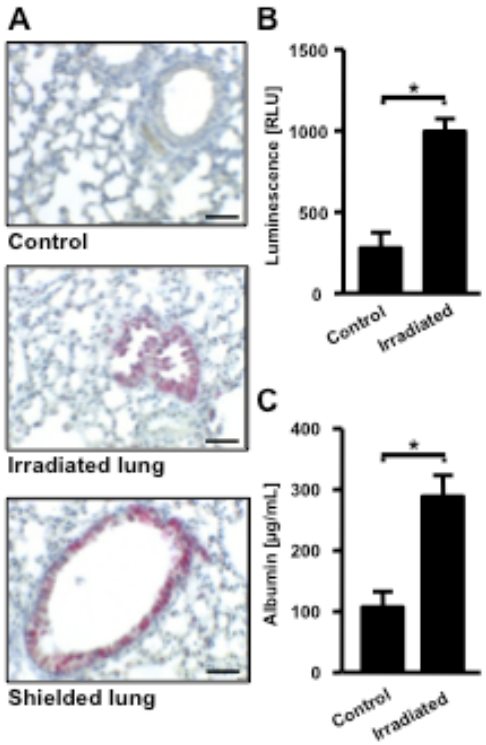
A
Control
Irradiated lung
Shielded lung
B
Luminescence [RLU]
1500
1000
500
0
*
Control
Irradiated
C
Albumin [µg/mL]
400
300
200
100
0
*
Control
Irradiated

Figure 2

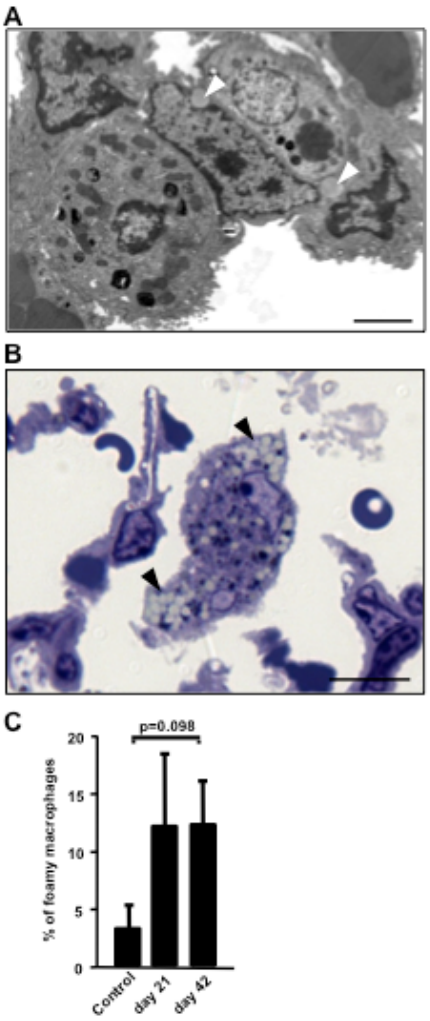
A
B
C
p=0.098
% of foamy macrophages
20
15
10
5
0
Control
day 21
day 42

Figure 3

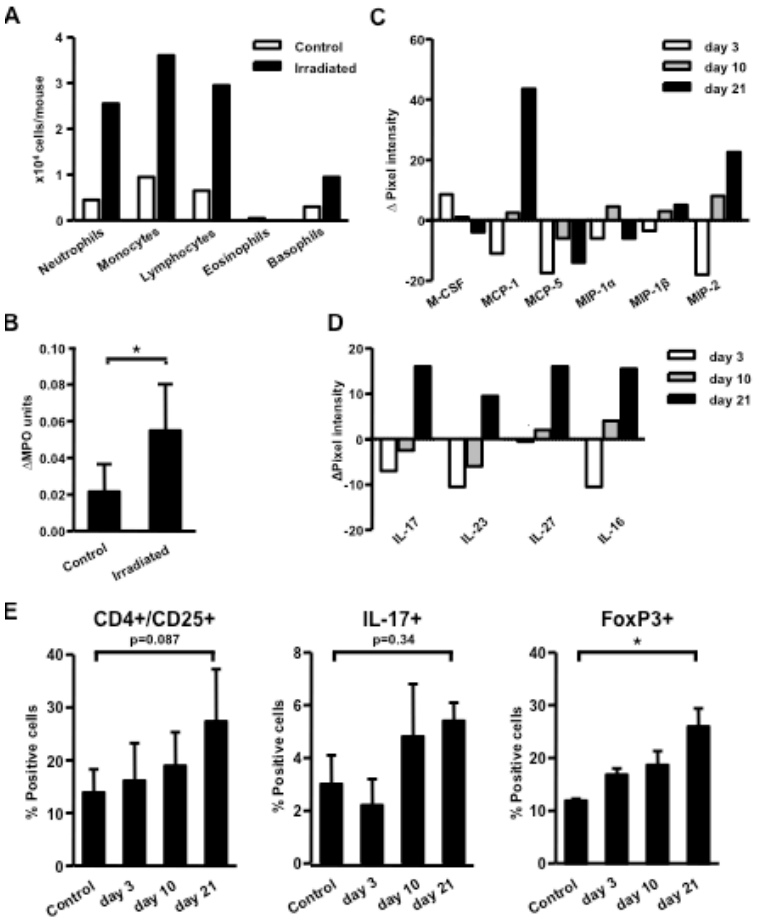
A
Control
Irradiated
x10⁴ cells/mouse
Neutrophils
Monocytes
Lymphocytes
Eosinophils
Basophils
C
day 3
day 10
day 21
Δ Pixel intensity
M-CSF
MCP-1
MCP-5
MIP-1α
MIP-1β
MIP-2
B
*
ΔMPO units
Control
Irradiated
D
day 3
day 10
day 21
ΔPixel intensity
IL-17
IL-23
IL-27
IL-16
E
CD4+/CD25+
p=0.087
% Positive cells
Control
day 3
day 10
day 21
IL-17+
p=0.34
% Positive cells
Control
day 3
day 10
day 21
FoxP3+
*
% Positive cells
Control
day 3
day 10
day 21

Figure 4

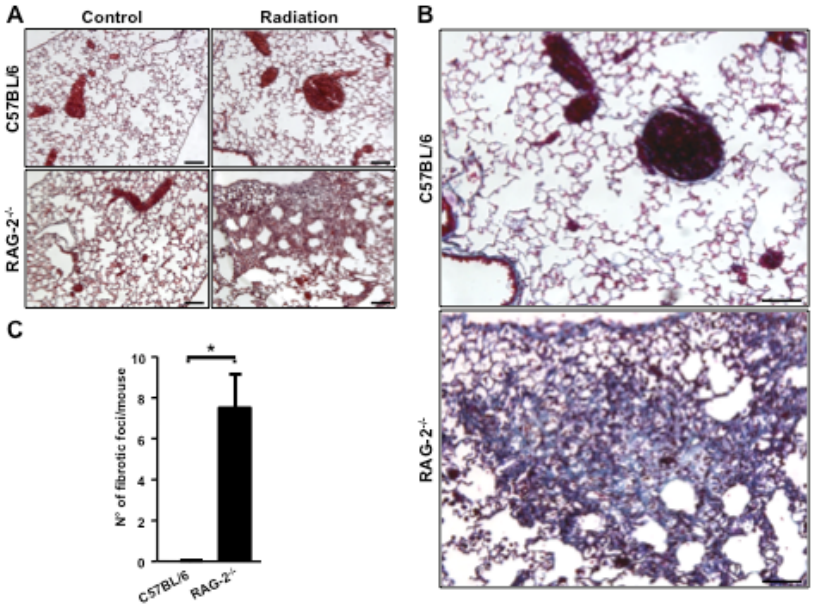
A
Control
Radiation
C57BL/6
RAG-2-/-
B
C57BL/6
RAG-2-/-
C
N° of fibrotic foci/mouse
10
8
6
4
2
0
*
C57BL/6
RAG-2-/-